Bioorganic & Medicinal Chemistry 18 (2010) 8112–8118

Contents lists available at ScienceDirect

Bioorganic & Medicinal Chemistry

journal homepage: www.elsevier.com/locate/bmc

Structural insights into the hot spot amino acid residues of mushroom tyrosinase for the bindings of thujaplicins

Satoshi Takahashi [a], Takanori Kamiya [b], Kazunori Saeki [c], Tomoka Nezu [c], Shin-ichiro Takeuchi [b], Ryoko Takasawa [c], Satoshi Sunaga [a], Atsushi Yoshimori [a], Shigeo Ebizuka [b], Takehiko Abe [b], Sei-ichi Tanuma [c,d,*]

[a] Institute for Theoretical Medicine, Inc., 4259-3 Nagatsuda-cho, Midori-ku, Yokohama 226-8510, Japan
[b] Hinoki Shinyaku Co., Ltd, 9-6 Nibancho, Chiyoda-ku, Tokyo 102-0084, Japan
[c] Department of Biochemistry, Faculty of Pharmaceutical Sciences, Tokyo University of Science, 2641 Yamazaki Noda, Chiba 278-8510, Japan
[d] Genome and Drug Research Center, Tokyo University of Science, 2641 Yamazaki Noda, Chiba 278-8510, Japan

ARTICLE INFO

Article history:
Received 27 July 2010
Revised 27 August 2010
Accepted 28 August 2010
Available online 12 October 2010

Keywords:
Tyrosinase
Thujaplicins
Hot spot
Homology modeling
MM-GB/SA
Free energy decomposition analysis

ABSTRACT

Tyrosinase inhibitors are important agents for cosmetic products. We examined here the inhibitory effects of three isomers of thujaplicins (α, β and γ) on mushroom tyrosinase and analyzed their binding modes using a homology model from the crystal structure of *Streptomyces castaneoglobisporus* tyrosinase (PDB ID: 1wx2). All the thujaplicins were found to be competitive inhibitors and γ-thujaplicin has the most potent inhibitory activity (IC_{50} = 0.07 μM). It is noted that there are good correlations between their observed IC_{50} values and their binding free energies calculated by MM-GB/SA. The binding modes of thujaplicins were predicted to be similar to that of Tyr98 of caddie protein (ORF378), which was co-crystallized with *S. castaneoglobisporus* tyrosinase. Furthermore, free energy decomposition analysis indicated that the potent inhibitory activity of γ-thujaplicin is due to the interactions with His242, Val243 and Pro257 (hot spot amino acid residues) at the active site of tyrosinase. These results provide a novel structural insight into the hot spot of mushroom tyrosinase for the specific binding of γ-thujaplicin.

1. Introduction

Tyrosinase (EC 1.14.18.1) is a copper-containing, mixed-function oxidase which is widely distributed in organisms.[1] This enzyme catalyzes both the hydroxylation of monophenols and the oxidation of *o*-diphenols into *o*-quinones.[2] Two cupric ions individually connected with three histidine residues at the active site are directly involved in the different catalytic activities via oxy-, deoxy- and met-states.[3,4] The quinone product is a reactive precursor for the synthesis of melanin pigments. In mammals, tyrosinase is responsible for skin pigmentation defects and abnormalities such as flecks.[5] Recently, this enzyme was reported to link to Parkinson's and other neurodegenerative diseases.[6,7] Furthermore, in plants, tyrosinase causes browning effects on vegetables, fruits and mushrooms.[8]

For several decades, tyrosinase inhibitors have become critical agents in cosmetic, agricultural and medicinal products.[9,10] A number of tyrosinase inhibitors such as arbutin, kojic acid, L-ascorbic acid, hinokitiol (β-thujaplicin) and phenylthiourea, from both natural and synthetic sources have been identified.[11,12] Kojic acid is the most intensively studied inhibitor of tyrosinase, and used as a cosmetic skin-whitening agent and as a food additive for preventing enzymatic browning.[13] It acts as a good chelator of transition metal ions such as a cupric ion,[14] and is a competitive inhibitor of mushroom tyrosinase.[15] However, the use for cosmetics is limited, because of its insufficient inhibitory activity, instability and cytotoxicity. Although many kojic acid derivatives, such as glycoside[16] and amino acid conjugates,[17] have been tried to synthesize to improve its unsuitable properties, it is still required to develop potent, specific and safety inhibitors of tyrosinase.

The crystal structure of tyrosinase from *Streptomyces castaneoglobisporus* has been reported in 2006,[18] enabling a better understanding of its mechanism of action. The structural analysis revealed the presence of a hydrophobic protein pocket adjoining the binuclear copper active site and has opened up the way for molecular modeling and a structure-based platform for design of novel inhibitors.

The aim of this work is to investigate hot spot amino acid residues at the active site of mushroom tyrosinase for the binding of thujaplicins. Thujaplicins are a series of related chemical substances isolated from *Thuja* plicate tree and exist as three

Abbreviations: MM-GB/SA, molecular mechanics-generalized born/surface area; SASA, solvent-accessible surface area; GB, generalized born.

* Corresponding author. Tel.: +81 4 7124 1501 (6470); fax: +81 4 7121 3620.
E-mail address: tanuma@rs.noda.tus.ac.jp (S. Tanuma).

0968-0896/$ - see front matter © 2010 Elsevier Ltd. All rights reserved.
doi:10.1016/j.bmc.2010.08.056

structural isomers, α-thujaplicin, β-thujaplicin (hinokitiol) and γ-thujaplicin. This is the first report that among the thujaplicins, γ-thujaplicin is the most potent competitive inhibitor. MM-GB/SA calculation by using the homology model of mushroom tyrosinase showed that the binding free energy of γ-thujaplicin is the lowest in this series. Furthermore, decomposition analysis of the binding free energy indicated that the potent inhibitory activity of γ-thujaplicin is due to the specific interactions with His242, Val243 and Pro257 (hot spot amino acid residues) at the active site of tyrosinase. On the other hand, the most contributed residue for the interaction of the substrate, L-tyrosine, with tyrosinase was predicted to be Asp255 at the active site. These structural insights into the unique interaction of γ-thujaplicin with tyrosinase may be useful for screening and design of novel specific and potent inhibitors of tyrosinase.

2. Results

2.1. Inhibitory activities of thujaplicins against tyrosinase

The effects of α-, β- and γ-thujaplicins on mushroom tyrosinase activity were examined by measuring the hydroxylation of L-tyrosine. Kojic acid and β-thujaplicin (hinokitiol) were selected as positive control compounds, since their inhibitory activities were already reported.[12] As shown in Figure 1, all the thujaplicins inhibit tyrosinase activity in a dose-dependent manner. The concentrations to inhibit 50% of tyrosinase activity (IC_{50}) are summarized in Table 1. γ-Thujaplicin was found to be the most potent inhibitor (IC_{50} = 0.07 μM) among the thujaplicins. The IC_{50} values of β- and α-thujaplicins were 0.09 and 9.53 μM, respectively. The inhibitory effect of γ-thujaplicin was approximately two-orders of magnitude stronger than that of α-thujaplicin. These results indicate that the position of isopropyl group attached to the cycloheptatrienolone (thujaplicin skeleton) is the main concern to the difference of inhibitory activities.

In order to solve the mode of inhibition of tyrosinase by thujaplicins, their inhibition kinetics were analyzed by Lineweaver-Burk plot analysis (Fig. 2). In the presence of 0.02 and 0.06 μM γ-thujaplicin, the same V_{max} value of 0.06 ΔA_{475}/min and the different K_m values of 0.53 and 0.95 mM, respectively, were obtained (Fig. 2C and Table 2). Thus, γ-thujaplicin is suggested to be a competitive inhibitor of tyrosinase with the K_i value of 0.02 μM (Table 2). As

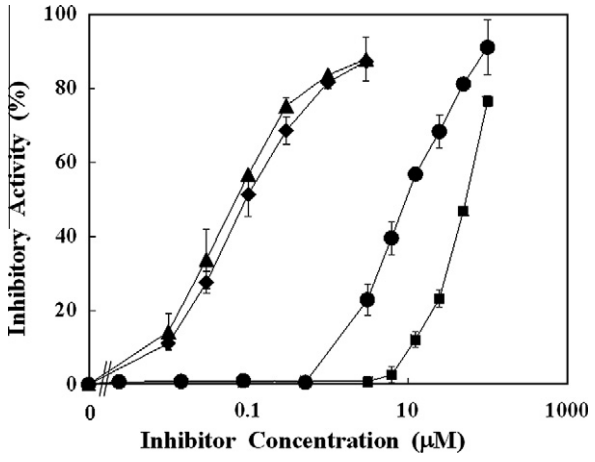

Figure 1. Effects of thujaplicins on mushroom tyrosinase activity. Tyrosinase activity was measured using L-tyrosine as the substrate as described under Section 4. Data were shown as the percentage of inhibition by α-thujaplicin (*circle*), β-thujaplicin (*diamond*), γ-thujaplicin (*triangle*) and kojic acid (*square*). The data are the averages of three independent experiments and bars show the S.D. values.

Table 1
Tyrosinase inhibitory activities of thujaplicins and kojic acid

Structure	Compound	IC_{50} (μM)
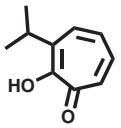	α-Thujaplicin	9.53
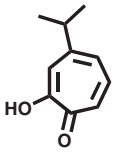	β-Thujaplicin	0.09
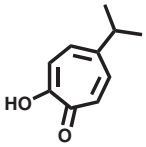	γ-Thujaplicin	0.07
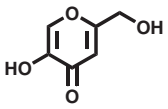	Kojic acid	53.70

shown in Figure 2A and B, α- and β-thujaplicins are also competitive inhibitors with the K_i values of 3.30 and 0.06 μM, respectively (Table 2). These observations suggest that thujaplicins bind to the same active site as the substrate, L-tyrosine. The comparison of the binding modes of three isomer thujaplicins with tyrosinase will provide important implications for understanding of the most potent inhibitory activity of γ-thujaplicin.

2.2. Computational 3D structure model of tyrosinase

The coordinate of the crystal structure of *S. castaneoglobisporus* tyrosinase (PDB ID: 1wx2) was used as a template in the molecular modeling of mushroom tyrosinase. *S. castaneoglobisporus* tyrosinase has been co-crystallized with ORF378, which is called caddie protein because of its carrying cupric ions for tyrosinase.[18] Caddie protein places a Tyr98 residue at the active site of tyrosinase. The phenol ring of Tyr98 is stacked with the imidazole ring of His242. The crystal structure suggested that Tyr98 of caddie protein functions as a competitive inhibitor to the substrate, L-tyrosine.

The alignments of *S. castaneoglobisporus* and mushroom tyrosinase sequences revealed 21% sequence identity and 39% sequence similarity within the catalytic domains (Fig. 3A).[18] The active site of *S. castaneoglobisporus* tyrosinase contains two cupric ions (Cu^A and Cu^B); Cu^A binds to Nε nitrogen atoms of His45, His69 and His78, and Cu^B binds to those of His238, His242 and His270. These histidine residues are conserved in the primary amino acid sequence of mushroom tyrosinase (Fig. 3A). The alignments were supplied along with the 3D coordinates of the template as an input to the program MODELLER9v3,[19] and the 3D model of mushroom tyrosinase was built by ligand-supported homology modeling including L-tyrosine, which modified from Tyr98 of caddie protein, two cupric ions and peroxide ion (Fig. 3B).

To validate the reliability of the homology model, it was evaluated using the program RAMPAGE,[20] which is a structure validation tool for the assessment of the Ramachandran plot of protein. As the results, the rate of residues in favoured and allowed regions was 96%, while the rate of residues in outlier region was 4% (Fig. 3C). The residues in outlier region did not locate at the active site of tyrosinase. Thus, we conclude that the homology model is reliable and able to use for in silico work.

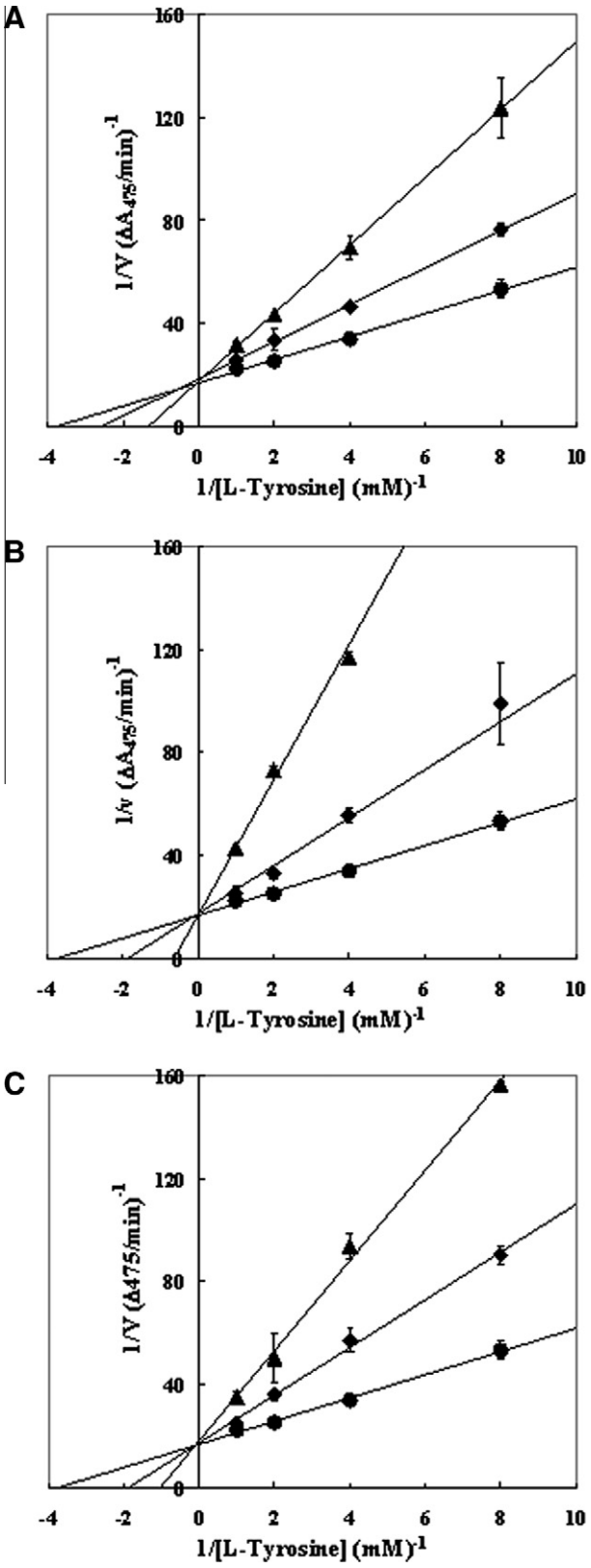

Figure 2. Lineweaver-Burk plots of mushroom tyrosinase reaction in the presence or absence of (A) α-thujaplicin, (B) β-thujaplicin and (C) γ-thujaplicin. Data were obtained as mean values ± S.D. of 1/*V*, inverse of the increase of absorbance at a wavelength 475 nm per min (ΔA_{475}/min), of three independent tests with different concentrations of L-tyrosine as a substrate. Inhibitors were (A) α-thujaplicin with 6 μM (*triangle*), 3 μM (*diamond*) or no α-thujaplicin (*circle*), (B) β-thujaplicin with 0.2 μM (*triangle*), 0.05 μM (*diamond*) or no β-thujaplicin (*circle*), and (C) γ-thujaplicin with 0.06 μM (triangle), 0.02 μM (diamond) or no γ-thujaplicin (*circle*).

Table 2
Kinetic parameters of tyrosinase in the presence of thujaplicins

Compound	K_i (μM)	Dose (μM)	K_m (mM)
α-Thujaplicin	3.3	0	0.0.26
		3.00	0.38
		6.00	0.74
β-Thujaplicin	0.06	0	0.26
		0.05	0.53
		0.20	1.16
γ-Thujaplicin	0.02	0	0.26
		0.02	0.53
		0.06	0.95

2.3. Binding modes of thujaplicins with tyrosinase

In order to understand the binding modes of thujaplicins with mushroom tyrosinase, they were docked at the active site of tyrosinase using Autodock program[21] as described under Section 4. The lowest scoring poses of all the docking runs were chosen as the binding modes. The superimposition of the binding modes for γ-thujaplicin and L-tyrosine is depicted in Figure 3D. The binding mode of γ-thujaplicin indicated the chelating of the carbonyl and hydroxyl groups of cycloheptatrienolone with two cupric ions at the active site of the tyrosinase, as the hydroxyl group of L-tyrosine (Fig. 3D). α- and β-thujaplicins were superimposed onto the binding mode of γ-thujaplicin.

The binding free energies of thujaplicins were calculated by using MM-GB/SA method.[22–24] As the results, the binding free energies of α-, β- and γ-thujaplicins were calculated to be −17.23, −22.37 and −24.40 kcal/mol, respectively (Table 3). The binding free energy of γ-thujaplicin was the lowest in this series. In addition, the binding free energy of L-tyrosine calculated by the MM-GB/SA method was −21.06 kcal/mol (Table 3). This value is near to that of β-thujaplicin. It is noted that there are good correlations between the binding free energies and the observed IC_{50} values (Table 2).

2.4. Analysis of hot spot amino acid residues on tyrosinase

In order to examine hot spot amino acid residues at the active site of tyrosinase, free energy decomposition analysis was performed using Amber 9.[25–28] As shown in Figure 4A, the most contributed residue is Pro257 (free energy = −2.38 kcal/mol) for γ-thujaplicin, and the second contributed residue is His242 (free energy = −2.27 kcal/mol) (Fig. 4A). In α- and β-thujaplicins, almost the same decomposition patterns were observed (Fig. 4A). The binding modes indicated that cycloheptatrienolone of thujaplicins forms stacking interactions with imidazole ring of His242 and cyclopentyl ring of Pro257 (Fig. 4B). Therefore, the interactions of thujaplicins with tyrosinase are suggested to be attributed to two main factors: chelating effects of two cupric ions and stacking interactions with His242 and Pro257.

The third contributed residue is Val243 (free energy = −0.80 kcal/mol) for γ-thujaplicin (Fig. 4A). The binding mode indicated that the isopropyl group of γ-thujaplicin locates in direction to Val243, and could form hydrophobic interaction with Val243 (Fig. 4B). The isopropyl group of β-thujaplicin could also form hydrophobic interaction with Val243, and the free energy is −0.71 kcal/mol (Fig. 4A and B). On the other hand, the isopropyl group of α-thujaplicin locates far from direction to Val243, and the free energy is −0.22 kcal/mol (Fig. 4A and B). Thus, the main reason for higher inhibitory activity of γ-thujaplicin than that of α- or β-thujaplicins is considered to be the hydrophobic interaction of the isopropyl group with Val243. Furthermore, these results suggest that interactions with His242, Pro257 and Val243 are necessary for potent inhibitory activity of thujaplicins. Thus, we define

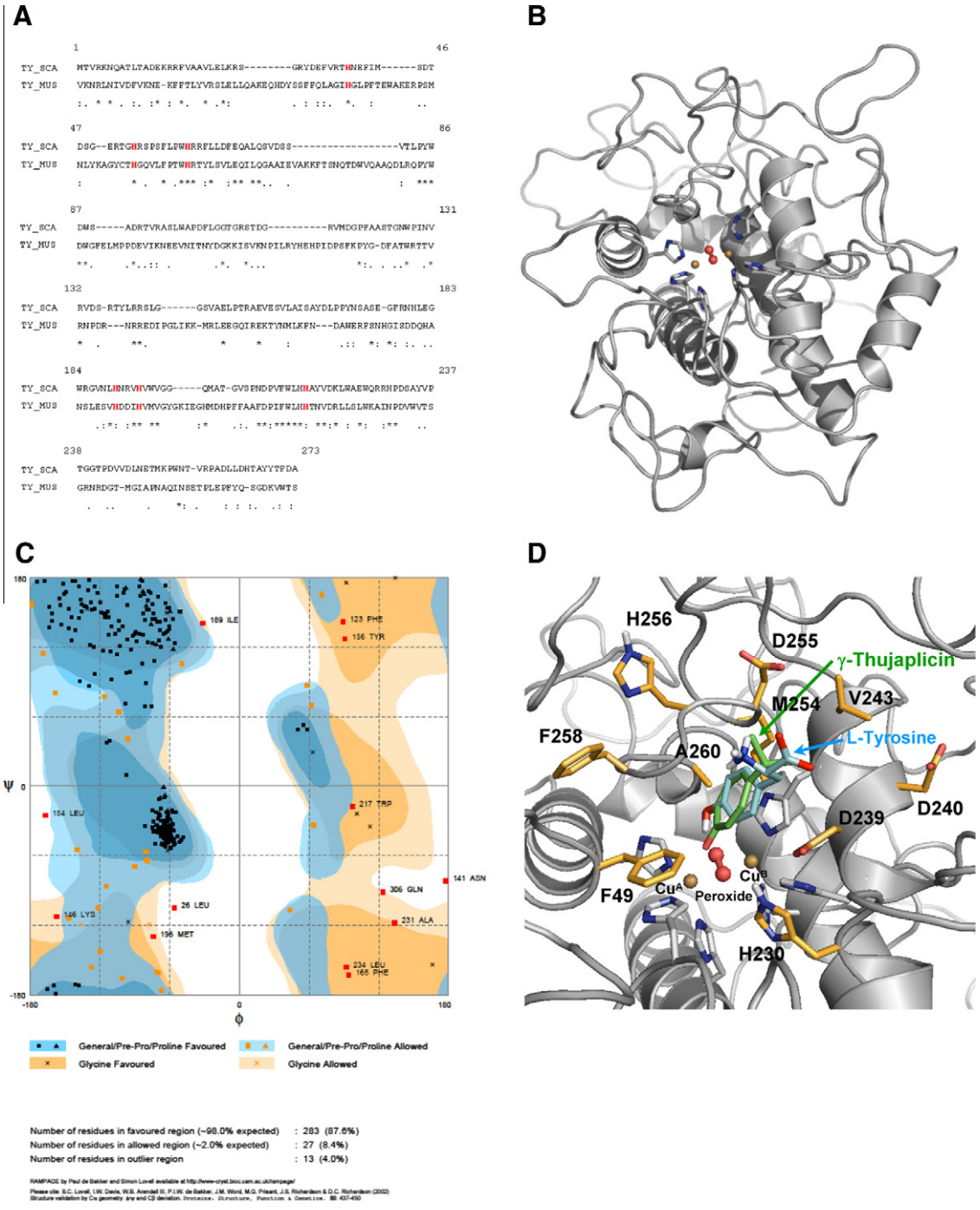

Figure 3. Homology modeling for mushroom tyrosinase and binding pose with thujaplicins. (A) Sequence alignments of *Streptomyces castaneoglobisporus* and mushroom tyrosinases. *TY_SCA* and *TY_MUS* indicate the amino acid sequence of the *Streptomyces castaneoglobisporus* and mushroom tyrosinase, respectively. The asterisks and the dots indicate identical and similar residues, respectively. The red bold letters indicate the His residues participating in copper binding. (B) Homology model of mushroom tyrosinase. Sand balls are two cupric ions. Red ball and stick is peroxide ion. (C) Ramachandran plot of the psi/phi distribution of the homology model as obtained by RAMPAGE: 96.0% residues are in favoured and allowed regions and 4.0% residues are in outlier region. (D) Superimposition of L-tyrosine modified from Tyr98 of caddie protein (ORF378) onto docking pose of γ-thujaplicin. Carbon atoms of the L-tyrosine, γ-thujaplicin and the flexible residues defined for docking are illustrated in cyan, lime and orange sticks, respectively. Hydrogen, oxygen and nitrogen atoms are illustrated in white, red and blue sticks, respectively.

Table 3
Binding free energies of thujaplicins by MM-GB/SA calculation

Compound	IC_{50} (mM)	MM-GB/SA (kcal/mol)
α-Thujaplicin	9.53	−17.23
β-Thujaplicin	0.09	−22.37
γ-Thujaplicin	0.07	−24.40
L-Tyrosine	—	−21.06

these residues (His242, Val243 and Pro257) as the hot spot amino acid residues at the active site of tyrosinase.

The free energy decomposition analysis of the substrate, L-tyrosine, whose binding mode forms a hydrogen bond with carbonyl oxygen of the main-chain of Asp255 in tyrosinase (Fig. 4C), was performed. As shown in Figure 4A, the most contributed residue for L-tyrosine is Asp255 (free energy = −2.29 kcal/mol). It is

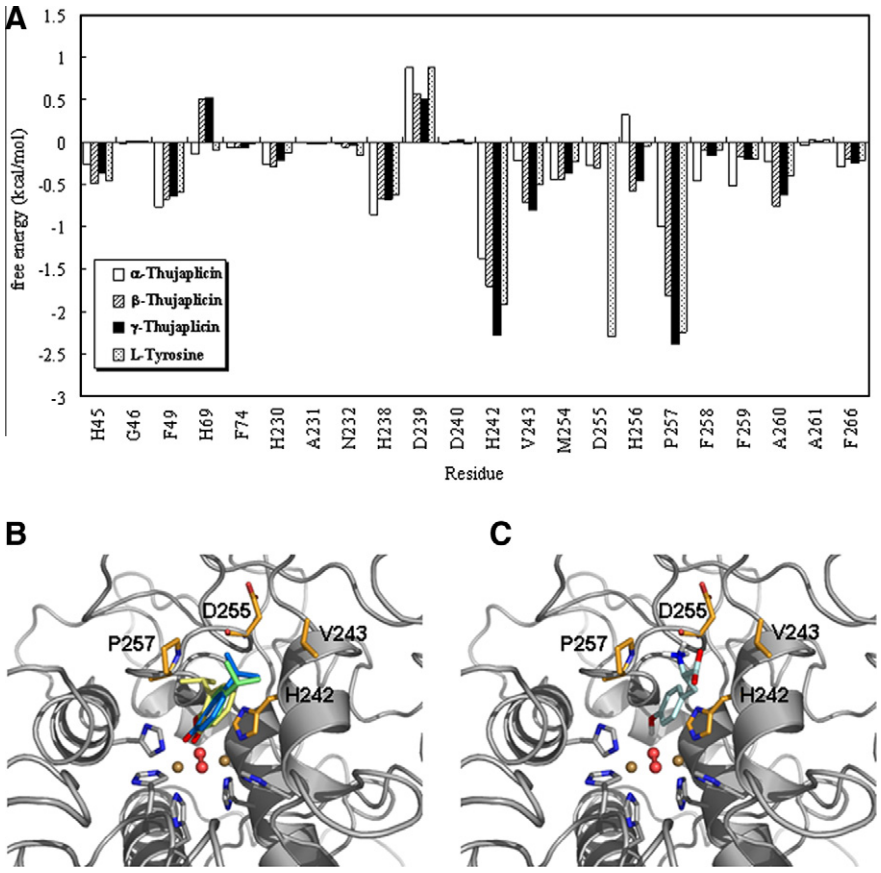

Figure 4. Free energy decomposition analysis and the binding modes of thujaplicins and L-tyrosine. (A) Decomposition of ΔG_{bind} on a per-residue within 7 Å from thujaplicins. (B) Binding modes of thujaplicins. Carbon atoms of the α-, β- and γ-thujaplicins are illustrated in pale yellow, marine and lime sticks, respectively. Carbon atoms of the hot spot amino acid residues (H242, V243 and P257) and D255 are illustrated in orange sticks. Hydrogen, oxygen and nitrogen atoms are illustrated in white, red and blue sticks, respectively. (C) Binding modes of L-tyrosine. Carbon atoms of the L-tyrosine are illustrated in cyan sticks. Carbon atoms of the hot spot amino acid residues (H242, V243 and P257) and D255 are illustrated in orange sticks. Hydrogen, oxygen and nitrogen atoms are illustrated in white, red and blue sticks, respectively.

interesting that Asp255 does not involve in the interactions of thujaplicins with tyrosinase.

3. Discussion

As tyrosinase become more important target in cosmetic, agricultural and medicinal fields, the development of tyrosinase inhibitors with higher bioactivities and lower side effects is required. Identification of the hot spot amino acid residues at the active site of tyrosinase is necessary to develop rationally specific and potent inhibitors. In this study, three thujaplicin isomers were used for getting structural insights into the hot spot amino acid residues of tyrosinase. We found that γ-thujaplicin (IC_{50} = 0.07 μM) is the most potent inhibitor among thujaplicins. In kinetics studies, all the thujaplicins were appeared to be competitive inhibitors. These data suggest that the binding site of thujaplicins to tyrosinase is the same active site as the substrate (L-tyrosine) binding. Furthermore, there are good correlations between the observed IC_{50} values and the binding free energies of thujaplicins by MM-GB/SA calculation, and their binding modes are similar to that of L-tyrosine. This supports the specific interaction of γ-thujaplicin at the active site of tyrosinase.

By using the free energy decomposition analysis, we could predict three amino acids (His242, Val243 and Pro257) as hot spot residues. On the other hand, the free energy decomposition analysis of the substrate, L-tyrosine, showed that the most contributed residue is Asp255 (free energy = −2.29 kcal/mol). Interestingly, Asp255 does not involve in the interactions of thujaplicins with tyrosinase. Thus, Asp255 is an important residue to consider a possible way for designing of more potent inhibitors. The information derived from these computational analyses provides a tool for predicting inhibitory activities of related compounds and for guiding further structural optimization of new types of tyrosinase inhibitors.

Since the mushroom tyrosinase is a cytosolic enzyme while the human tyrosinase is a membrane-bound enzyme,[29] the hot spot amino acid residues predicted here have some limitations to develop specific inhibitor of the human tyrosinase. Moreover, until now a little study with purified human tyrosinase has been performed. Using purified human tyrosinase and its homology model will open up the way for developing novel tyrosinase inhibitors for human. Although traditional cosmetic ingredients for tyrosinase inhibitor used to be limited to mainly plant extracts, hydrolysates and essential oils etc., from now on, it will be possible to generate safety inhibitors rationally designed by hot spot analysis of the human tyrosinase.

4. Materials and methods

4.1. Materials

Mushroom tyrosinase and L-tyrosine were purchased from Sigma. Kojic acid (5-hydroxy-2-(hydroxymethyl)-4*H*-pyran-4-one) was purchased from Tokyo Kasei Kogyo Co. Ltd. α-Thujaplicin (2-hydroxy-3-isopropyl-2,4,6-cycloheptatrien-1-one), β-thujaplicin (2-hydroxy-4-isopropyl-2,4,6-cycloheptatrien-1-one) and γ-thujaplicin (2-hydroxy-5-isopropyl-2,4,6-cycloheptatrien-1-one) were

purchased from Osaka Organic Chemical Industry Ltd and were of analytical grade (purity ⩾ 95%).

4.2. Measurement of tyrosinase activity

Tyrosinase activity was measured as previously described[30,31] with slight modifications. Five microliter of 500 unit/mL mushroom tyrosinase, 19 μL of 50 mM potassium phosphate buffer (pH 6.5) and 1 μL of test sample were incubated at 30 °C for 5 min, and then 25 μL of 2 mM L-tyrosine was added. The mixture was incubated at 30 °C for 15 min and absorbance at 475 nm was continuously monitored with a SpectraMax Plus384 (Molecular Device). The percentage of inhibition of tyrosinase activity was calculated as follows: % Inhibition = $(1 - A/B) \times 100$, where A is the initial slope of absorbance of 475 nm versus time with the tested sample and B is the initial slope of absorbance of 475 nm versus time with DMSO instead of the sample. Kojic acid was used as a positive inhibition standard. The concentration required to inhibit tyrosinase activity by 50% is defined as the IC_{50} value. The Michaelis–Menten constant (K_m), maximal velocity (V_{max}) and the inhibition constant (K_i) were determined by Lineweaver-Bulk plot with various concentrations of L-tyrosine as a substrate.

4.3. Homology modeling of mushroom tyrosinase

The coordinate of the crystal structure of *S. castaneoglobisporus* tyrosinase (PDB ID: 1wx2), which is obtained from the Protein Data Dank (PDB),[32] was used as a template to construct the initial homology model of mushroom tyrosinase. Sequence alignment data between *S. castaneoglobisporus* and mushroom tyrosinase referred the paper of Ref. 18. In this study, we carried out ligand-supported homology modeling which generates homology models including two cupric ions, peroxide ion and L-tyrosine of the active sites. The construction of homology model based on the alignment was performed using MODELLER9v3.[19] The substrate tyrosine was constructed by superimposing Tyr98 of caddie protein. Two cupric ions, peroxide ion, L-tyrosine and six histidine residues (His45, His69, His78, His238, His242 and His270) at the active site of tyrosinase were fixed those coordinates. Ten models were generated by *automodel class* of MODELLER9v3. Best model was selected according to the lowest DOPE (Discrete Optimized Protein Energy) score.[33] In addition, a loop region (Tyr142-Phe171) of the selected model was refined by using *loopmodel class* in MODDELLER9v3. During the refinement of loop region, the coordinates of other regions were fixed. The homology model was estimated by RAMPAGE.[20]

4.4. Prediction of binding modes of thujaplicins with tyrosinase

The thujaplicins were constructed by CS ChemDraw Ultra and CS Chem3D Ultra, and optimized to their minimum energy with the MOPAC program[34] and the AM1 semiempirical Hamiltonian.

The docking compatible structure formats of the homology model were prepared by AutoDockTools-1.5.4, an accessory program that allows the user to interact with AutoDock from a graphic user interface. Non-polar hydrogen atoms were merged and Gastiger atomic charges assigned. The solvation parameters were added by the Addsol program. In addition, we defined residues within 7 Å of the substrate tyrosine (Phe49, His230, Asp239, Asp240, Val243, Met254, Asp255, His256, Phe258 and Ala260) as the flexible residues except Pro257 and histidine residues at the active site of tyrosinase. The grid points were set to the catalytic site of the enzyme by the AutoGrid program. The number of grid points in *xyz* was set to 40, 40, 40, the spacing value equivalent to 0.250 Å, and the grid center to −14.813, −17.903, 22.226. Ligand docking was carried out with the AutoDock4.2[21] Lamarckian Genetic Algorithm (GA). The approximate binding free energies calculated by this program are based on an empirical function, derived by linear regression analysis of protein–ligand complexes with known binding constants. This function includes terms for changes in energy due to van der Waals, hydrogen bonds and electrostatic forces, as well as ligand torsion and desolvation. The docked energy also includes the ligand internal energy or the intramolecular interaction energy of the ligand. All of the docking parameters were assigned the default values. Rotational bonds in the ligand were assigned with the program AutoTors program. Simulation was performed a total of 10 times.

We attempted to construct energy-minimized binding modes of thujaplicins in the presence of the two cupric ions and peroxide ion using Amber 9.[25–28] However the van der Waals parameters of cupric ion are absence by default in parm99 force field.[35] So, the van der Waals parameters of cupric ion set $R = 1.27$ Å and $E = 0.06$ kcal/mol,[36] and the nonbonded model for cupric ion was constructed.[37] Thereafter, binding modes of thujaplicins were energy minimized by 500 steps of steepest descent minimization followed by 500 steps of conjugate gradient minimization in vacuo. The harmonic restraints with force constants of 100 kcal/(mol Å^2) applied to two cupric ions, peroxide ion and atoms of six histidine residues at the active site.

4.5. MM-GB/SA and free energy decomposition analysis

The binding free energies for thujaplicins/tyrosinase interactions were calculated by MM-GB/SA method[22–24] in Amber 9.[20–23] In this method, the binding free energies are calculated for predicted binding modes of thujaplicins. The binding free energy (ΔG_{bind}) is calculated as the sum of the energetic contributions, which correspond to the molecular mechanical gas-phase energies ($E_{MM} = E_{elec} + E_{vdw}$) and the solvation free energies (ΔG_{solv}), plus the entropic contributions ($-T\Delta S$). The molecular mechanical energies were evaluated using an infinite cutoff for nonbonded interactions. The solvation free energies (ΔG_{solv}) were estimated as the sum of an electrostatic solvation energy (G_{polar}), calculated with the generalized Born model,[38] plus a nonpolar solvation energy ($G_{nonpolar}$), proportional to the solvent-accessible surface area, which includes the entropy cost of creating a solute-sized cavity in the solvent.[38] G_{polar} was calculated using the Hawkins, Cramer, Truhlar pairwise GB model[39,40] using the parameters developed by Tsui et al.[41], and the values of the interior and the exterior dielectric constants were set to 1 and 80, respectively. $G_{nonpolar}$ was calculated from solvent accessible surface area determined by the ICOSA method: $G_{nonpolar} = 0.0072 \times SASA$. In the ICOSA method, the surface area is computed by recursively approximating a sphere around an atom, starting from icosahedra. The entropic term is found to be much smaller than the other two terms (E_{MM} and ΔG_{solv}) in many applications of estimating relative binding free energies.[42] Because thujaplicins show similar chemical structure, we neglected entropic terms in this study.

The free energy decomposition analysis using the MM-GB/SA was performed by *mm_pbsa module* of Amber 9 for tyrosinase residues. The detailed description of MM-GB/SA decomposition procedure used in Amber was reported by Gohlke et al.[43] The free energy decomposition based on MM-GB/SA is only a pragmatic way to estimate the contribution of each residue to protein–ligand interactions.

Acknowledgment

We would like to thank Daniel Koekert for critical comments and fruitful discussions.

References and notes

1. Sánchez-Ferrer, A.; Rodríguez-López, J. N.; García-Cánovas, F.; García-Carmona, F. *Biochim. Biophys. Acta* **1995**, *1247*, 1.
2. Chen, Q.; Liu, X.; Huang, H. *Biochemistry (Mosc)* **2003**, *68*, 644.
3. Decker, H.; Tuczek, F. *Trends Biochem. Sci.* **2000**, *25*, 392.
4. Fenoll, L. G.; Peñalver, M. J.; Rodríguez-López, J. N.; Varón, R.; García-Cánovas, F.; Tudela, J. *Int. J. Biochem. Cell Biol.* **2004**, *36*, 235.
5. Oetting, W. S. *Pigment Cell Res.* **2000**, *13*, 320.
6. Xu, Y.; Stokes, A. H.; Roskoski, R. J.; Vrana, K. E. *J. Neurosci. Res.* **1998**, *54*, 691.
7. Asanuma, M.; Miyazaki, I.; Ogawa, N. *J. Neurotox. Res.* **2003**, *5*, 165.
8. Artés, F.; Castañer, M.; Gil, M. I. *J. Agric. Food Chem.* **1998**, *4*, 377.
9. Fitzparick, T. B.; Eisen, A. Z.; Wolff, K.; Freedberg, I. M.; Austen, K. F. *Dermatology in general medicine*, New York, NY, 1983.
10. Maeda, K.; Fukuda, M. *J. Soc. Cosmet. Chem.* **1991**, *42*, 361.
11. Te-Sheng, C. *Int. J. Mol. Sci.* **2009**, *10*, 2440.
12. Sakuma, K.; Ogawa, M.; Sugibayashi, K.; Yamada, K.; Yamamoto, K. *Arch. Pharm. Res.* **1999**, *22*, 335.
13. Chen, J. S.; Wei, C.; Marshall, M. R. *J. Agric. Food Chem.* **1991**, *39*, 1897.
14. Kahn, V.; Ben-Shalom, N.; Zakin, V. J. *J. Agric. Food Chem.* **1997**, *45*, 4460.
15. Kim, Y. M.; Yun, J.; Lee, C.-K.; Min, K. R.; Kim, Y. *J. Biol. Chem.* **2002**, *18*, 16340.
16. Nishimura, T.; Kometani, T.; Takii, H.; Terada, Y.; Shigetaka, O. *J. Ferment. Bioeng.* **1994**, *1*, 37.
17. Noh, J. M.; Kwak, S. Y.; Seo, H. S.; Seo, J. H.; Kim, B. G.; Lee, Y. S. *Bioorg. Med. Chem. Lett.* **2009**, *19*, 5586.
18. Matoba, Y.; Kumagai, T.; Yamamoto, A.; Yoshitsu, H.; Sugiyama, M. *J. Biol. Chem.* **2006**, *13*, 8981.
19. Sali, A.; Blundell, T. L. *J. Mol. Biol.* **1993**, *234*, 779.
20. Lovell, S. C.; Davis, I. W.; Arendall, W. B., III; de Bakker, P. I. W.; Word, J. M.; Prisant, M. G.; Richardson, J. S.; Richardson, D. C. *Proteins: Struct. Funct. Genet.* **2003**, *50*, 437.
21. Morris, G. M.; Goodsell, D. S.; Halliday, R. S.; Huey, R.; Hart, W. E.; Belew, R. K.; Olson, A. J. *J. Comput. Chem.* **1998**, *19*, 1639.
22. Lee, M. R.; Duan, Y.; Kollman, P. A. *Proteins: Struct. Funct. Genet.* **2000**, *39*, 309.
23. Wang, J.; Morin, P.; Wang, W.; Kollman, P. A. *J. Am. Chem. Soc.* **2001**, *123*, 5221.
24. Swanson, J. M. J.; Henchman, R. H.; McCammon, J. A. *Biophys. J.* **2004**, *86*, 67.
25. Case, D. A.; Darden, T. A.; Cheatham, T. E., III; Simmerling, C. L.; Wang, J.; Duke, R. E.; Luo, R.; Merz, K. M., Jr.; Pearlman, D. A.; Crowley, M.; Walker, R. C.; Zhang, W.; Wang, B.; Hayik, S.; Roitberg, A. E.; Seabra, G.; Wong, K. F.; Paesani, F.; Wu, X.; Brozell, S.; Tsui, V.; Gohlke, H.; Yang, L.; Tan, C.; Mongan, J.; Hornak, V.; Cui, G.; Beroza, P.; Mathews, D. H.; Schafmeister, C.; Ross, W. S.; Kollman, P. A. *AMBER 9*; University of California: San Francisco, 2006.
26. Pearlman, D. A.; Case, D. A.; Caldwell, J. W.; Ross, W. S.; Cheatham, T. E., III; DeBolt, S.; Ferguson, D.; Seibel, G.; Kollman, P. A. *Comput. Phys. Commun.* **1995**, *91*, 1.
27. Case, D. A.; Cheatham, T. E., III; Darden, T. A.; Gohlke, H.; Luo, R.; Merz, K. M., Jr.; Onufriev, A.; Simmerling, C. L.; Wang, B.; Woods, R. *J. Comput. Chem.* **2005**, *26*, 1668.
28. Cornell, W. D.; Cieplak, P.; Bayly, C. I.; Gould, I. R., Jr.; Ferguson, D.; Pellmeyer, D. C.; Fox, T.; Cadwell, J. W.; Kollman, P. A. *J. Am. Chem. Soc.* **1995**, *117*, 5179.
29. Parvez, S.; Kang, M.; Chung, H. S.; Bae, H. *Phytother. Res.* **2007**, *21*, 805.
30. Pomerantz, S. H.; Li, J. P.-H.. In *Methods Enzymology*; Tabor, H., Tabor, C. W., Eds.; Academic Press: New York, 1970; Vol. 37, pp 620–626.
31. Prota, G.; Ortonne, J.; Voulot, C.; Khatchadourian, C.; Nardi, G.; Palumbo, A. *Comp. Biochem. Physiol. B* **1981**, *68*, 415.
32. Berman, H. M.; Westbrook, J.; Feng, Z.; Gilliland, G.; Bhat, T. N.; Weissig, H.; Shindyalov, I. N.; Bourne, P. E. *Nucleic Acids Res.* **2000**, *28*, 235.
33. Shen, M. Y.; Sali, A. *Protein Sci.* **2006**, *15*, 2507.
34. Stewart, J. J. *J. Comput. Aided Mol. Des.* **1990**, *4*, 1.
35. Cieplak, P.; Caldwell, J.; Kollman, P. *J. Comput. Chem.* **2001**, *22*, 1048.
36. Soliman, K.; Ohad, N.; Ramadan, M.; Snait, T.; Tal, P.; Jacob, V. *J. Med. Chem.* **2007**, *50*, 2676.
37. Stote, R. H.; Karplus, M. *Proteins* **1995**, *23*, 12.
38. Still, W. C.; Tempczyk, A.; Hawley, R. C.; Hendrickson, T. *J. Am. Chem. Soc.* **1990**, *112*, 6127.
39. Hawkins, G. D.; Cramer, C. J.; Truhlar, D. G. *J. Phys. Chem.* **1996**, *100*, 19824.
40. Hawkins, G. D.; Cramer, C. J.; Truhlar, D. G. *Chem. Phys. Lett.* **1995**, *246*, 122.
41. Tsui, V.; Case, D. A. *Nucl. Acid Sci.* **2001**, *56*, 275.
42. Srinivasan, J.; Cheatham, T. E.; Cieplak, P.; Kollman, P. A.; Case, D. A. *J. Am. Chem. Soc.* **1998**, *120*, 9401.
43. Gohlke, H.; Kiel, C.; Case, D. A. *J. Mol. Biol.* **2003**, *330*, 891.